On some features of the eigenvalue problem for the PN approximation of the neutron transport equation

On some features of the eigenvalue problem for the P_N approximation of the neutron transport equation

Nicolò Abrate[a], Sandra Dulla[a,b], Piero Ravetto[a,b], Paolo Saracco[c]

[a] *Politecnico di Torino, Dipartimento Energia, Corso Duca degli Abruzzi, 24 - 10129 Torino (Italy)*
[b] *I.N.F.N. - Sezione di Torino - Via P. Giuria, 1 - 10125 Torino (Italy)*
[c] *I.N.F.N. - Sezione di Genova, Via Dodecaneso, 33 - 16146 Genova (Italy)*

Abstract

In this work some characteristics of the eigenvalue problem for the neutron transport equations are considered. Various formulations are examined, discussing some theoretical and practical aspects. The standard multiplication eigenvalue that is particularly relevant for nuclear reactor physics applications is analysed, together with the time eigenvalue, including also the contribution of delayed neutrons. In addition, the less common collision and density eigenvalues are also discussed, highlighting interesting physical features. A semianalytical approach is developed allowing to evidence some interesting structures of the eigenvalue spectra.
The study is carried out within the spherical harmonics approach. For the plane one dimensional geometry, the mathematical relationship between even and odd-order approximations for the homogeneous form of the equations for the eigenvalue formulation is investigated. It is shown that the even-order system of equations can be re-cast in the form of the contiguous lower odd-order one. Numerical results are obtained in the two-group energy model for various configurations for which a reference is available, providing also results for high-order approximations. The study includes a presentation and discussion of the spectra patterns for the various eigenvalue formulations.

Email addresses: nicolo.abrate@polito.it (Nicolò Abrate), sandra.dulla@polito.it (Sandra Dulla), piero.ravetto@polito.it (Piero Ravetto), paolo.saracco@ge.infn.it (Paolo Saracco)

Keywords: P_N approximation, spherical harmonics, eigenvalue problems, neutron transport equation

---

Foreword by Piero Ravetto

With the death of Massimo Salvatores our community lost a giant. All those who scientifically interacted with him could immediately realize that he was no ordinary scientist. Moreover, all those who had the privilege to know him in person beyond the professional field can attest that he had also extraordinary human qualities. And he will be sorely missed by all.

Massimo visited Politecnico di Torino many times over the years, to give seminars, short courses or just to meet. The first time I invited him, he gave a short course on actinide transmutation and on sensitivity analysis, many years before these topics became hot issues. He will be always remembered for his outstanding contributions to the studies on the practical applications of nuclear energy, but he also contributed significantly to several aspects of theoretical reactor physics and to neutron transport theory. He never disowned his original mathematical and physical background, as he earned a degree in physics at the University of Torino. He was also fond of the beauty of mathematical elegance.

This work with which my younger colleagues and I wish to contribute to give honour to his memory addresses some basic mathematical and physical aspects of the spectrum of the neutron transport equation. When meeting, we often discussed on the importance of fully understanding the mathematical subtleties of neutron transport, especially for the education of young researchers. Within the enormous corpus of his scientific production one can find various papers on such very fundamental topics.

I personally want to express my deep gratitude to Massimo for his enduring friendship and, at last, for coming to my retirement party at the International Conference on Transport Theory held in Paris in September 2019 and I am honoured to have treated him for a beer afterwards. Unfortunately, that was also the last time I met him.

1. Introduction

The determination of the eigenvalues and eigenfunctions of the neutron transport equation is one of the fundamental problems in nuclear reactor

physics. Eigenvalues and eigenfunctions provide an important physical insight into the characteristics of a multiplying system and are very useful for various applications in both steady-state and dynamic conditions. For realistic systems their determination requires sophisticate numerical techniques. However, the solution of the eigenproblem for simple configurations allows to understand the physical features of the transport model adopted.

In a recent paper [1], various formulations of the eigenproblem were presented and discussed within the spherical harmonics approach to the neutron transport equation. In that study a convergence assessment was carried out, allowing to investigate some peculiar properties of even and odd-order approximations from a novel point of view. A further paper [2] is investigating the possibility to use methods for the acceleration of the process to reach a high-quality benchmark accuracy in the results, validated by Monte Carlo, which might, therefore, be useful as a reliable reference for numerical techniques.

The spherical harmonics methodology (often referred to as the P_N approximation [3]) is used also in this work that extends and completes the analysis previously performed. As the interest is mainly analytical, methodological and didactic, only the one-dimensional planar geometry is here considered. At first, the relationship between odd and even-order approximations is discussed for the eigenproblem, showing how it is possible to cast the set of differential equations for an even-order approximation into the same form as the equations for the preceding odd-order, by suitably linearly combining the unknown moments and redefining the coefficients. Afterwards, the various formulations of the eigenproblem are considered. The interest is especially focused on the energy features, analysing the multigroup model and presenting numerical results for the two-group case.

The eigenvalue problem has been given various formulations along the history of neutron transport. All the different formulations are physically interesting, as they may highlight some specific features of the transport process and are all mathematically useful and attractive in order to understand the intricate mathematics connected to the transport equation. For instance, among other applications, Massimo Salvatores used reactor harmonics for the investigation of the degree of decoupling of a system and for the exploitation of higher-order forms of perturbation theory [4].

For standard nuclear engineering applications, mainly the classic multiplication eigenvalue k has been used, as it can be directly connected to the approach to reach criticality through the adjustment of the multiplica-

tive properties of the material constituting the nuclear reactor [5]. More recently, the time eigenvalue α has attracted some attention, owing to its strict connection to the time evolution of a non-critical system, in particular to its asymptotic behaviour when considering the fundamental one [6]. The α eigenvalue can be introduced in association to the Laplace transform of the transport equation. If the important effect of the delayed emissions is also considered, a more complicated eigenvalue model is obtained by application of the Laplace transform, where the eigenvalue appears in a non-linear form strictly related to the theory of omega-modes [7]. This model is worth studying, as it is of great interest for the rich physical information that can be retrieved for nuclear reactor kinetics applications and for the interpretation of neutronic experiments.

More exotic forms of the eigenvalue problem have also been proposed over the years, since, in principle, it can be assumed the eigenvalue modifies any term appearing in the transport equation. The collision eigenvalue is assumed to modify all the emission terms, both scattering and fission [8]; the density eigenvalue modifies all the terms involving a neutron collision [9]. Although these two formulations are mathematically well founded, they have not attracted much interest from the engineering community and are seldom considered. Very limited investigations on their physico-mathematical significance are thus available. In this paper, also these eigenvalues are considered.

2. Mathematical model

The general form of the integro-differential neutron transport model, including fission delayed emissions from R precursor families, is given by the following system of equations:

$$
\begin{cases}
\dfrac{1}{\mathrm{v}}\dfrac{\partial\phi(\vec{r},E,\hat{\Omega},t)}{\partial t}+\vec{\nabla}\cdot\Big(\vec{\Omega}\phi(\vec{r},E,\hat{\Omega},t)\Big)+\Sigma(\vec{r},E)\phi(\vec{r},E,\hat{\Omega},t)= \\
\quad\displaystyle\int dE'\oint d\hat{\Omega}'\,\Sigma_s(\vec{r},E')\phi(\vec{r},E',\hat{\Omega}',t)f_s(\vec{r},E'\longrightarrow E,\vec{\Omega}\cdot\vec{\Omega}')+ \\
\quad(1-\beta)\dfrac{\chi_p(\vec{r},E)}{4\pi}\displaystyle\int dE'\oint d\vec{\Omega}'\,\nu\Sigma_f(\vec{r},E')\phi(\vec{r},E',\hat{\Omega}',t)+ \\
\quad\displaystyle\sum_{i=1}^{R}\dfrac{\chi_i(\vec{r},E)}{4\pi}\lambda_i C_i(\vec{r},t)+S(\vec{r},E,\hat{\Omega},t) \\
\\
\dfrac{\partial C_i(\vec{r},t)}{\partial t}=\beta_i\displaystyle\int dE'\oint d\hat{\Omega}'\,\nu\Sigma_f(\vec{r},E')\phi(\vec{r},E',\hat{\Omega}',t)-\lambda_i C_i(\vec{r},t), \\
\quad i=1,\ldots,R,
\end{cases}
\tag{1}
$$

where the symbols here and in the following have their standard meaning, as defined in all nuclear reactor physics books [5, 10]. The eigenvalue is introduced when taking the steady-state form of this system of equations and eliminating the external source. For the purpose of a compact writing, it is convenient to introduce the following operators:
the streaming operator

$$\hat{T}=\vec{\nabla}\cdot\Big(\hat{\Omega}\,*\Big)\,; \tag{2}$$

the removal by collision operator

$$\hat{\Sigma}=\Sigma(\vec{r},E)*; \tag{3}$$

the scattering operator

$$\hat{C}=\int dE'\oint d\hat{\Omega}'\,\Sigma_s(\vec{r},E)f_s(\vec{r},E'\longrightarrow E,\vec{\Omega}\cdot\vec{\Omega}')*; \tag{4}$$

the prompt fission operator

$$\hat{F}_p=(1-\beta)\frac{\chi_p(\vec{r},E)}{4\pi}\int dE'\oint d\vec{\Omega}'\,\nu\Sigma_f(\vec{r},E')*; \tag{5}$$

the delayed fission operator for the i^{th} delayed precursor family

$$\hat{F}_i = \beta_i \frac{\chi_i(\vec{r}, E)}{4\pi} \int dE' \oint d\hat{\Omega}' \, \nu\Sigma_f(\vec{r}, E') *; \tag{6}$$

the total fission operator

$$\hat{F} = \hat{F}_p + \sum_{i=1}^{R} \hat{F}_i; \tag{7}$$

the net loss operator .

$$\hat{L} = \hat{T} + \hat{\Sigma} - \hat{C} \, . \tag{8}$$

Assuming a steady-state situation, the delayed neutron precursor balance equations can be solved and back-substituted into the neutron balance equation. Eliminating the source, the following two eigenvalue formulations can be obtained:
the multiplication eigenvalue (effective multiplication factor) k equation,

$$\hat{L}\phi = \frac{1}{k}\hat{F}\phi; \tag{9}$$

and the collision or γ-eigenvalue equation,

$$\left(\hat{T} + \hat{\Sigma}\right) \phi = \frac{1}{\gamma} \left(\hat{C} + \hat{F}\right) \phi \, . \tag{10}$$

Alternatively, the so-called time eigenvalue α can be introduced in the balance equation:

$$\hat{T}\phi + \left(\hat{\Sigma} + \frac{\alpha}{\mathrm{v}}\right) \phi = \left(\hat{C} + \hat{F}\right) \phi, \tag{11}$$

where the term α/v amounts to a modification of the capture cross section and should therefore denoted as *time capture*, rather than the most common *time absorption*, which would also involve a modification of the operators appearing in the right-hand side. In equation (11), the total fission operator $\hat{F}$ is considered: physically, this means that the energy aspect of delayed neutrons is accounted for, but they are assumed to be emitted at the same time of the fission event.

If the delayed neutrons are explicitly included in the time formulation of the problem, the delayed neutron precursor equations need to be Laplace

transformed and the concentrations back substituted into the neutron transport equation. This operation leads to the following time eigenvalue ω equation:

$$\hat{T}\phi + \left(\hat{\Sigma} + \frac{\omega}{\mathtt{v}}\right)\phi = \hat{C}\phi + \hat{F}_p\phi + \sum_{i=1}^{R} \frac{\lambda_i}{\omega + \lambda_i}\hat{F}_i\phi\,. \tag{12}$$

A further eigenvalue equation can be obtained supposing the eigenvalue to act on all terms that contain a macroscopic cross section, thus effectively acting on the density of the material constituting the system where neutrons are diffusing. This leads to the δ eigenvalue equation:

$$\hat{T}\phi = \frac{1}{\delta}\left(\hat{C} + \hat{F} - \hat{\Sigma}\right)\phi\,. \tag{13}$$

The question arises on the significance of such an artificial operation introduced to reach a steady-state solution. A first observation that might help in the physical interpretation of the numerical results presented in the following can be made noticing that both the production (scattering and fission) and the removal (total collision) terms are modified by the same factor, thus introducing a "competition" between positive and negative contributions. Quite differently, the δ factor may be regarded as a modification of the streaming term, leaving all the other terms unaltered. This action appears to be a modification of the relationship between the angular current ($\hat{\Omega}\phi$) and the angular flux. Alternatively, one can view this action as operating a re-scaling of the spatial coordinates. In other words, the eigenvalue is acting to modify the free-flight kernel of the transport process, as it can be easily verified by constructing the spatial integral form of the integro-differential equation (13), with standard mathematical procedures [11].

2.1. P_N equations: one- and two-group models

As anticipated, in this article the spherical harmonics P_N approximation [3] for a homogeneous one-dimensional plane system shall be studied: it is thus worth to report the basic formulae that constitute the model, at least in the one- and two-group energy group approaches that are used in this work.

In the one-group case, the angular flux shall depend only on one spatial coordinate x and on the cosine of the azimuthal angle μ, $\phi(x, \mu)$. Such flux is represented as a truncated series of Legendre polynomials, namely:

$$\phi(x, \mu) = \sum_{n=0}^{N} \frac{2n+1}{2}\phi_n(x)P_n(\mu)\,. \tag{14}$$

Consequently, the streaming and scattering terms take the form:

$$\begin{aligned}\hat{T}\phi &= \mu\frac{\partial}{\partial x}\sum_{n=0}^{N}\frac{2n+1}{2}\phi_n(x)P_n(\mu)\\ &= \sum_{n=0}^{N}\frac{2n+1}{2}\frac{d\phi_n(x)}{dx}\frac{(n+1)P_{n+1}(\mu)+nP_{n-1}(\mu)}{2n+1}\end{aligned} \tag{15}$$

and

$$\hat{C}\phi = \sum_{n=0}^{N}\frac{2n+1}{2}\Sigma_s f_n\phi_n(x)P_n(\mu) \tag{16}$$

where f_n are the moments of the scattering function, explicitly defined as:

$$f_n \equiv \int d\mu_0 f_s(\mu_0)P_n(\mu_0)\,. \tag{17}$$

To simplify notation, it is worth setting the following definitions:

$$\begin{aligned}\Sigma_n &= \Sigma_s f_n\\ F_n &= \nu\Sigma_f(1-\beta)\delta_{n\,0}\\ D_{i\,n} &= \nu\Sigma_f\beta_i\delta_{n\,0}\,, \qquad i=1,2,\ldots,R\,.\end{aligned} \tag{18}$$

All the eigenvalue problems presented above can be included in the following system of $N+1$ differential equations:

$$\begin{aligned}&\varepsilon_\delta\left[\frac{n+1}{2n+1}\frac{d\phi_{n+1}(x)}{dx}+\frac{n}{2n+1}\frac{d\phi_{n-1}(x)}{dx}\right]+\left(\Sigma+\frac{\varepsilon_\alpha}{\mathtt{v}}\right)\phi_n(x)=\\ &\varepsilon_\gamma\left[\Sigma_n+\varepsilon_k\left(F_n+\sum_{i=1}^{R}\frac{\lambda_i}{\lambda_i+\varepsilon_\omega}D_{i\,n}\right)\right]\phi_n(x),\ n=0,\ldots,N,\end{aligned} \tag{19}$$

where the values of the ε parameters are given in Table 1.

It is easy to generalise the above formulation to multi-group. For instance, in the two-group case the two-dimensional vector flux shall take the form

$$\begin{aligned}&\vec{\phi}=\begin{pmatrix}\phi_1(x,\mu)\\ \phi_2(x,\mu)\end{pmatrix}=\sum_{n=0}^{N}\frac{2n+1}{2}\begin{pmatrix}\phi_{1,n}(x)\\ \phi_{2,n}(x)\end{pmatrix}P_n(\mu)=\\ &\sum_{n=0}^{N}\frac{2n+1}{2}\vec{\phi}_n(x)P_n(\mu).\end{aligned} \tag{20}$$

eigenvalue	critical value	ε_k	ε_α	ε_ω	ε_γ	ε_δ
k	1	$1/k$	0	0	1	1
α	0	1	α	0	1	1
ω	0	1	ω	ω	1	1
γ	1	1	0	0	$1/\gamma$	1
δ	1	1	0	0	1	δ

Table 1: The set of ε parameters to be used in eq. (19).

It is then possible to write the streaming and scattering terms as:

$$\hat{T} = \sum_{n=0}^{N} \frac{2n+1}{2} \frac{d}{dx} \begin{pmatrix} \phi_{1,n}(x) \\ \phi_{2,n}(x) \end{pmatrix} \frac{(n+1)P_{n+1}(\mu) + nP_{n-1}(\mu)}{2n+1}, \tag{21}$$

$$\hat{C} = \sum_{n=0}^{N} \frac{2n+1}{2} \begin{pmatrix} \Sigma_{1\to1} f_{1\to1,n} & 0 \\ \Sigma_{1\to2} f_{1\to2,n} & \Sigma_{2\to2} f_{2\to2,n} \end{pmatrix} \begin{pmatrix} \phi_{1,n}(x) \\ \phi_{2,n}(x) \end{pmatrix} P_n(\mu), \tag{22}$$

with obvious definitions for $f_{g'\to g,n}$.

For conciseness sake, the following matrix operators are introduced,

$$\begin{aligned} \hat{V} &= \begin{pmatrix} \frac{1}{\mathtt{v_1}} & 0 \\ 0 & \frac{1}{\mathtt{v_2}} \end{pmatrix} \\ \hat{\Sigma} &= \begin{pmatrix} \Sigma_1 & 0 \\ 0 & \Sigma_2 \end{pmatrix} \\ \hat{\Sigma}_n &= \begin{pmatrix} \Sigma_{1\to1} f_{1\to1,n} & 0 \\ \Sigma_{1\to2} f_{1\to2,n} & \Sigma_{2\to2} f_{2\to2,n} \end{pmatrix} \\ \hat{F}_n &= \begin{pmatrix} \nu_1\Sigma_{f,1}\chi_{p,1} & \nu_2\Sigma_{f,2}\chi_{p,1} \\ \nu_1\Sigma_{f,1}\chi_{p,2} & \nu_2\Sigma_{f,2}\chi_{p,2} \end{pmatrix} (1-\beta)\delta_{n0} \\ \hat{D}_{i,n} &= \begin{pmatrix} \nu_1\Sigma_{f,1}\chi_{i,1} & \nu_2\Sigma_{f,2}\chi_{i,1} \\ \nu_1\Sigma_{f,1}\chi_{i,2} & \nu_2\Sigma_{f,2}\chi_{i,2} \end{pmatrix} \beta_i\delta_{n0},\ i = 1, ..., R. \end{aligned} \tag{23}$$

The eigenvalue problems take the following form that generalises eq. (19):

$$\varepsilon_\delta \left[\frac{n+1}{2n+1} \frac{d\vec{\phi}_{n+1}(x)}{dx} + \frac{n}{2n+1} \frac{d\vec{\phi}_{n-1}(x)}{dx} \right] + \left(\hat{\Sigma} + \varepsilon_\alpha \hat{V} \right) \vec{\phi}_n(x) = \varepsilon_\gamma \left[\hat{\Sigma}_n + \varepsilon_k \left(\hat{F}_n + \sum_{i=1}^{R} \frac{\lambda_i}{\lambda_i + \varepsilon_\omega} \hat{D}_{i\,n} \right) \right] \vec{\phi}_n(x), \tag{24}$$

where the ε parameters are again given in table 1. In this work, the eigenvalue equations are numerically solved with a spatial discretisation based on finite differences as described in detail in [1].

2.2. The boundary conditions

In this work the classic boundary conditions proposed by Mark [12, 13] and by Marshak [14] are used. For the sake of completeness, they are briefly given in the following. A more detailed and thorough treatment and physical discussion of the problem of boundary conditions can either be found in the original works by Mark and Marshak or in various books, e.g. [3]. The solution of the P_N system of first-order differential equations introduces a finite number of degrees of freedom for the moments of the angular flux. It is therefore impossible to satisfy exactly the correct conditions for the transport solution that involve the angular flux for all the incoming directions. In the case of vacuum boundary, the angular flux should vanish for all $\mu > 0$ at a left boundary and for $\mu < 0$ at a right boundary. In the Marshak formalism, such a situation is approximated by making to vanish some half-range integral functionals of the angular flux, namely for a left boundary x=0:

$$\int_0^1 d\mu \phi(x=0,\mu) P_m(\mu) = 0, \text{ for } m = 1, 3, \dots \ . \tag{25}$$

It is worth noticing that this condition for m=1 yields a zero incoming partial current. In the Mark formalism, the angular flux is imposed to vanish for a selected set of directions, usually chosen as the roots μ_i of the Legendre polynomials $P_{N+1}(\mu)$, when N is odd. Therefore, for a left boundary:

$$\phi(x=0,\mu_i) = 0, \tag{26}$$

for all $\frac{N+1}{2}$ positive values of μ_i.

In the case of an even value of N, one can choose either the roots of the polynomial $P_{N+1}(\mu)$, excluding 0 (option A in the following) or the roots of $P_N(\mu)$ (option B). At last, it is worth mentioning that both boundary conditions lead to negative values of the angular flux at the boundary for some directions, which may significantly affect the results especially for optically thin systems.

3. Some analytical results

The study of eigenvalue spectra through discretisation of the spatial dependence has the great advantage in the possibility to use highly efficient numerical algorithms for matrix eigenvalue determination: these techniques have been widely employed in the past and in our previous paper, where also a vast bibliography can be found [1]. However, a well known side effect of discretisation is a distortion of the topological disposition of the eigenvalues in the complex plane and also the possible presence of spurious eigenvalues.

To give some insight on this topic we develop a semi-analytical approach to the study of α eigenvalues without spatial discretisation. However, the formal complications of the method make it practically useful only for the simplest, lower order P_N approximations, in contrast to the focus on high N we followed in [1].

The condition for the eigenvalues derives from imposing proper homogeneous boundary conditions to the general solution of the P_N system of differential equations, which, for the case of constant cross sections, is a linear combination of exponentials of the form $e^{q_j(\alpha)x}$. The arguments of the exponentials are given in terms of the solutions of the characteristic polynomial, which obviously depend on α (or, more in general, on the chosen eigenvalue). As we shall see, the knowledge of the explicit relation between the q's and α is a required starting point to find the α spectrum. The characteristic polynomial is given by the determinant of a tridiagonal matrix:

$$\det \begin{pmatrix} z-\Delta_0 & q & 0 & 0 & \dots & 0 \\ \frac{q}{3} & z-\Delta_1 & \frac{2q}{3} & 0 & \dots & 0 \\ 0 & \frac{2q}{5} & z-\Delta_2 & \frac{3q}{5} & & 0 \\ \vdots & \dots & \dots & \dots & \ddots & \\ 0 & 0 & \dots & 0 & \frac{Nq}{2N+1} & z-\Delta_{N-1} \end{pmatrix}, \qquad (27)$$

where we conveniently defined $z = \frac{\alpha}{\mathrm{v}} + \Sigma$ and $\Delta_n = \nu\Sigma_f\delta_{n0} + \eta_n\Sigma_s$. It is immediate to realise, by direct inspection, that the dependence of the allowed frequencies q_j on α is rather involved because the solution of an $N+1$ degree algebraic equation is required. Since it is not possible to find explicit expressions for the roots of polynomials of degree $N > 4$, the strategy we follow is then to find some approximated model in which the allowed q's and the eigenvalues can be explicitly determined; after that, we locally search

the true eigenvalues in the proximity of these approximated values, by means of well assessed numerical zero finding algorithms, like e.g. a combination of Newton and secant methods.

By inspection it appears evident that such simple model can be obtained if no scattering and no fission are present, i.e. for a purely absorbing system: in such a case all the Δ_j vanish and the characteristic polynomial of the P_N system reduces to

$$Q_N(q) = \det \begin{pmatrix} z & q & 0 & 0 & \dots & 0 \\ \frac{q}{3} & z & \frac{2q}{3} & 0 & \dots & 0 \\ 0 & \frac{2q}{5} & z & \frac{3q}{5} & & 0 \\ \vdots & \dots & \dots & \dots & \ddots & \\ 0 & 0 & \dots & 0 & \frac{Nq}{2N+1} & z \end{pmatrix} . \tag{28}$$

Such determinants can be evaluated by using the recurrence for the continuants of a tridiagonal matrix

$$Q_N = zQ_{N-1} - \frac{(N-1)^2}{(2N-3)(2N-1)} q^2 Q_{N-2} \qquad Q_0 = 1, Q_{-1} = 0, \tag{29}$$

yielding easily

$$Q_N = \frac{q^{N+1}}{C_{N+1}} P_{N+1}\left(\frac{z}{q}\right) , \qquad \text{where} \qquad C_{N+1} = \frac{2^N (3/2)_N}{(2)_N} , \tag{30}$$

in terms of the Pochhammer symbol $(a)_n = a(a+1)\cdots(a+n-1) = \Gamma(a+n)/\Gamma(a)$. According to this expression, the allowed values for q are expressible by the inverse of the zeros of the Legendre polynomials of order $N+1$, say $\xi_j^{(N)}$, multiplied by z: this is precisely the analytic approximate relation for the allowed values $q_j(\alpha)$ we are looking for; it is true for every value of N, through the (irrational) zeros of the Legendre polynomials,

$$q_j^{(N)}(\alpha) = \frac{\frac{\alpha}{\mathtt{v}} + \Sigma}{\xi_j^{(N)}} \quad \Longleftrightarrow \quad L_N\left(\xi_j^{(N)}\right) = 0 \, , \xi_j^{(N)} \neq 0 \, . \tag{31}$$

The equation for the α eigenvalues derives from the compatibility condition on the set of equations imposing proper homogeneous boundary conditions.

In the simplest case, the P_1 approximation using Mark boundary condition (BC)[1], we arrive at the condition

$$\cosh(qs)+\frac{5}{3}\sinh(qs)=0 \qquad \Longrightarrow \qquad \cosh(\sqrt{3}zs)+\frac{5}{3}\sinh(\sqrt{3}zs)=0 \quad (32)$$

for a slab of width $2s$. In such a simple case, by splitting the real and imaginary part $\alpha=\alpha_R+i\alpha_I$, we conclude that

$$\frac{\alpha_R}{\mathtt{v}}=-\Sigma-\frac{\log 2}{\sqrt{3}s}\,, \qquad \frac{\alpha_I}{\mathtt{v}}=\frac{n\pi}{\sqrt{3}s}\,, \tag{33}$$

because, remarkably, $\log 2=\tanh^{-1}\left(\frac{3}{5}\right)$. Then, the solution is found and all the allowed eigenvalues lie on a straight line parallel to the imaginary axis. We remark that two conditions enabled to find the results: (i) the existence of an explicit invertible relation $q(\alpha)$, and (ii) the ability to solve the algebraic equation (32). This second condition is difficult to be realized starting from $N=3$, because the equivalent of condition (32) will be of the form

$$\sum_{j=1}^{2N} c_j e^{q_j^{(N)}(\alpha)s}=0\,, \qquad j=1,\ldots,2N \tag{34}$$

for a slab of width $2s$ in an odd P_N scheme, as it can be verified by direct calculation; the real coefficients c_j depend on the specific form of the (vacuum) boundary condition that is employed. The solution for such a condition can be a very difficult task in a general case.

A trick is helpful to reach the goal, at least numerically. Mathematica® [15] is in fact able to solve equations of the form (34), *provided the* $q_j^{(N)}(\alpha)$ *are given in terms of rational numbers*. Then, we can approximate the zeros of the Legendre polynomials with rational expressions to find some approximation to the eigenvalues and then use them as starting points for a local numerical search. In principle this algorithm could be adopted for any N, but in practice the evaluation of the coefficients c_j may become very heavy.

For the results presented in the following, it is assumed that the half-thickness of the slab is $s=1$ mfp and the particle velocity is unitary. In Figure 1 we show the result of such algorithm for the P_7 approximation. It is

[1]For which some additional algebraic simplifications occur, being given for $\mu=\pm\frac{1}{\sqrt{3}}$

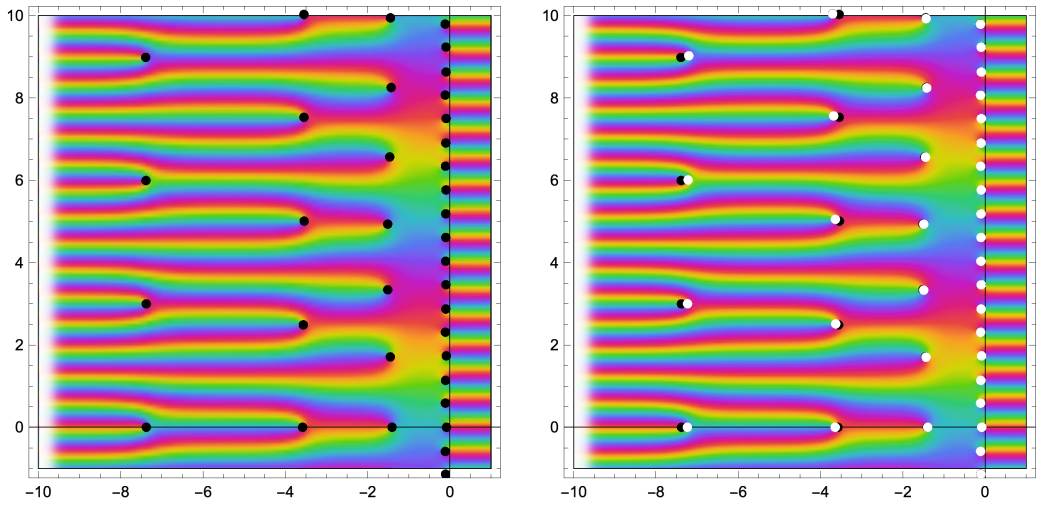

Figure 1: The approximated α-spectrum for the P_7 case in the complex z plane, when a two digit decimal approximation to the zeros of the Legendre polynomial is used (left, black dots); on the right, white dots show the positions of the numerically exact eigenvalues when only absorption is present. The coloured background is a plot of the argument of the complex function representing the eigenvalue condition, using a colour function spanning from $-\pi$ (yellow) to π (purple) counterclockwise around the zeros.

remarkable to observe that the solutions of the rational approximation to the eigenvalue condition lie on a set of $(N+1)/2$ lines parallel to the imaginary axis; our guess is that the same happens for any N also for the "exact" numerical results which are shown on the right side of the figure.

To conclude, we need to bring back interactions into the game: this can be done in the same way just shown before, but this time using as starting points for the search of the zeros the values obtained with the above procedure, which is effective only if the relation $q(\alpha)$ can be found. We show in Figures 2 and 3 the results for the P_1 and P_3 cases, respectively. In both cases, the analytical structure of the compatibility condition for the eigenvalues in the complex plane is more complicated when interaction is switched on: in P_1, for instance, the relation $q(z)$ changes as

$$q(z) = \pm\sqrt{3}\sqrt{z^2} \longrightarrow \pm\sqrt{3}\sqrt{z^2 - z\Delta_0}, \tag{35}$$

which implies a branch cut from $-\Delta_0$ to Δ_0. An even more involved relation

is valid in the P_3 case, namely:

$$q(z) = \pm \frac{\sqrt{90z^2 + 55z\Delta_0 \pm \sqrt{5}z\sqrt{864z^2 + 1224z\Delta_0 + 605\Delta_0^2}}}{3\sqrt{2}} \,. \tag{36}$$

As we noted in a previous paper it is clear from Figure 3 by confronting the positions of the true eigenvalues with the ones obtained with $\Delta_0 = 0$ how the presence of the interaction manifests itself into a sort of repulsion between different branches of the spectrum, in complete analogy to what happens for a system of coupled oscillators [1, 16]. It is also clear, by looking at the two plots at the centre and at the right, how this effect is ruled by the amount of the interactions itself: this should be expected, but it prevents us from concluding that the true eigenvalues also lie on a straight line, which is clearly not true. The fact that the eigenvalues are located on a straight line in this particular physical case has to be ascribed to the absence of scattering implying no angular redistribution of particles, thus decoupling the behaviour of particles moving in different directions. This coupling phenomenon recalls the physics of two interacting oscillators [16].

4. Even-odd reduction

There is a further relevant point that can be analytically explored: usually the P_N approximation is developed for odd orders, because it is commonly believed that even ones tend to be less accurate than the previous odd ones [17, 18]: from a purely mathematical point of view it should be observed that in the even case the system of P_N equations is only apparently an ordinary system of differential equations, but it can be shown to be really a differential-algebraic system of equations, which is a system that contains both differential and algebraic equations, or it is equivalent to such a form [19, 20]. This can be seen explicitly by simply considering the P_2 case that entails the system:

$$\begin{cases} \phi_1'(x) + a\phi_0' = & 0 \\ \frac{2}{3}\phi_2'(x) + \frac{1}{3}\phi_0' + \phi_1 = & 0 \\ \frac{2}{3}\phi_1'(x) + \phi_2(x) = & 0 \end{cases} , \tag{37}$$

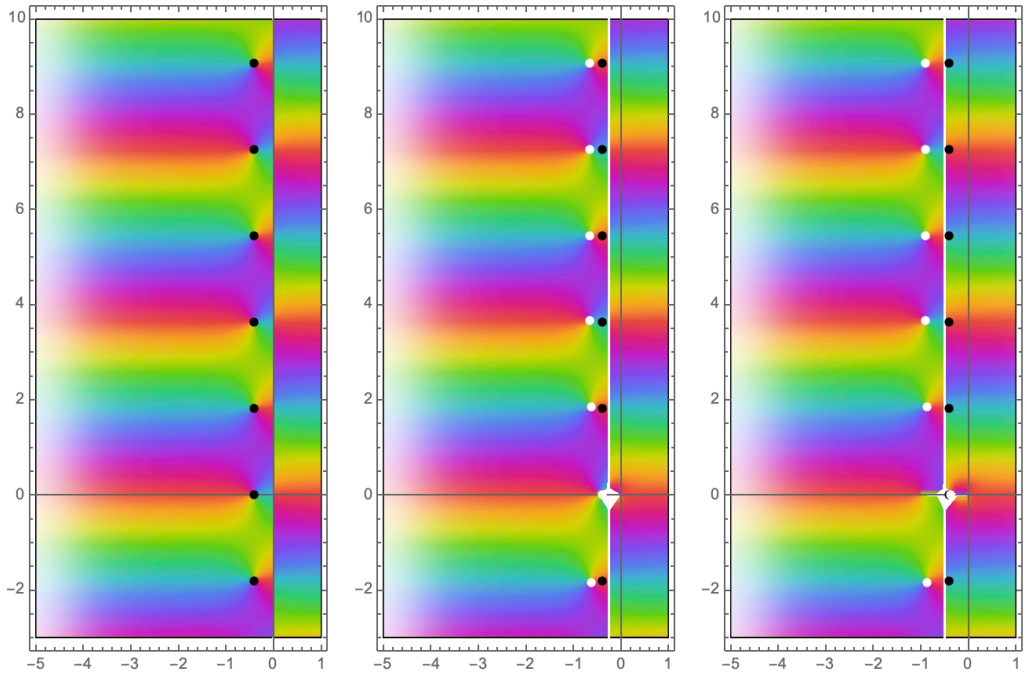

Figure 2: The approximated α-spectrum for the P_1 case in the complex z plane; left: $\Delta_0 = 0$, center: $\Delta_0 = 0.5$, right: $\Delta_0 = 1$. Black dots correspond to no scattering and no fission ($\Delta_0 = 0$), white dots are the numerical zeros. The coloured background is a plot of the argument of the complex function representing the eigenvalue condition, using the same colour code as in Figure 1.

where $a = \Sigma - \Delta_0$. By direct manipulation such a system reduces to

$$\begin{cases} \phi_1'(x) + a\phi_0' = & 0 \\ \left(\dfrac{4}{15}a + \dfrac{1}{3}\right)\phi_0' + \phi_1 = & 0 \\ -\dfrac{2}{5}a\phi_0(x) + \phi_2(x) = & 0 \end{cases}, \tag{38}$$

where two facts are made explicit: (i) the last equation is algebraic and simply amounts to a definition of ϕ_2 in terms of lower order moments, and (ii) the P_2 system is made equivalent to a P_1 model, with the replacement

$$\frac{1}{3} \longrightarrow \left(\frac{4}{15}a + \frac{1}{3}\right). \tag{39}$$

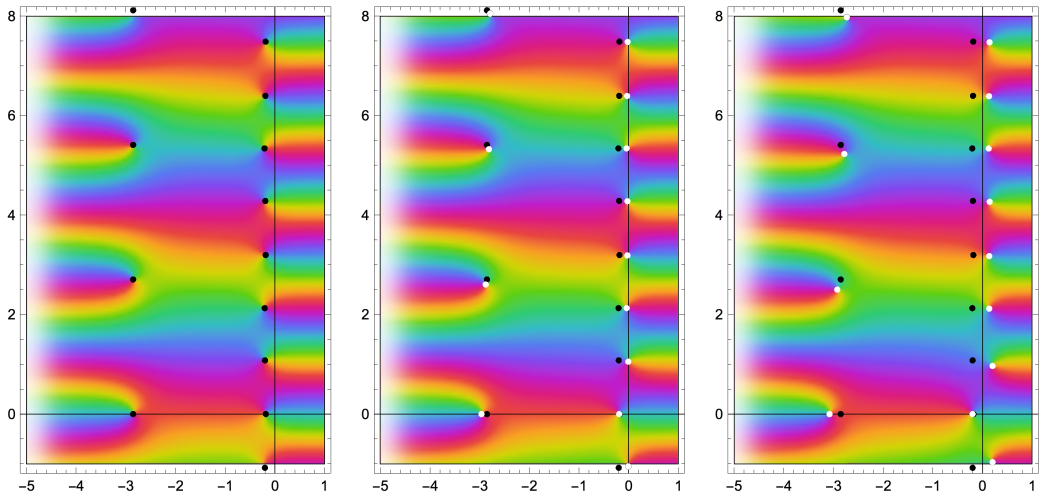

Figure 3: The approximated α-spectrum for P_3 in the complex z plane; left: $\Delta_0 = 0$, center: $\Delta_0 = 0.5$, right: $\Delta_0 = 1$. Black dots correspond to no scattering and no fission ($\Delta_0 = 0.$), white dots are the numerical zeros. The coloured background is a plot of the argument of the complex function representing the eigenvalue condition, using a the same colour code as in Figure 1.

In the usual P_1 approximation the coefficient multiplying ϕ_0' is related to the definition of the diffusion coefficient, so that equation (39) suggests the P_2 approximation is really equivalent to P_1, but with a different diffusion coefficient. It becomes then legitimate to ask if the same mechanism works also for higher-order even approximations, that is, if an even-order P_N approximation is effectively equivalent to an (odd) P_{N-1} with modified coefficients.

It is not difficult to show that this is indeed true, by using a similarity transformation, derived essentially by an algorithm similar to Gauss reduction. We give some examples of such algorithm in the case of pure isotropic scattering in the appendix: remarkably, such algorithm, which for higher values of N turns out to imply a recursion, is finite because the P_N system is represented by a lower triangular matrix.

The process begins by iteratively solving even-order equations with respect to the highest order moment derivative; in the P_4 case, for instance,

this leads to replacing the last ($m = 4$) equation with:

$$\phi_4(x) = -\frac{4}{9}\phi_3'(x) = \frac{4}{9}\frac{5}{3}\left(-\frac{2}{5}a\phi_0(x) + \phi_2(x)\right), \tag{40}$$

having previously solved $m = 0, 2$ equations as explained; then ϕ_4 results directly defined in terms of lower-order even moments. It is clear, by recursion, how this process works for every even-order approximation, because the sequence of (preceding) even equations enables to find all odd-order derivatives.

Then, after substituting the result for the highest order even angular flux moment into the previous $m = N - 1 = 3$ equation, one immediately recognizes that this is not in the required P_3-like form because of the presence of ϕ_0. However, one can now use the even equations to eliminate the unwanted term(s) iterating, if required; after this step has been performed the $m = 3$ equation really involves only ϕ_2, as it is in the form of the original P_3 system, with a different coefficient, as expected. Moreover, the equation contains not simply ϕ_3, but the combination

$$\Phi_3(x) = \phi_3(x) - \frac{4}{7}\frac{4}{9}2a\phi_0(x)\,. \tag{41}$$

This clearly suggests that it is convenient to introduce a new unknown function, by using the above equation. This replacement, which must be substituted back into the system, has the side effect of modifying also the $m = 2$ equation. Then, the suggested algorithm permits to recast the P_4 system into a P_3 form, with modified coefficients at the price of a redefinition of the unknowns through linear combination. This is quite obviously not a problem to our goal, because we can conclude that the P_4 approximation is really equivalent to a P_3 one with "effective" coefficients.

At higher values of N the same procedure applies, but it turns out that an iteration is involved because equations - and the corresponding redefinitions of the unknowns - are even-odd interleaved. Then, a redefinition of some fixed m flux moment involves not only lower index equation, but also the $(m+1)$-th one. One is thus led to an iteration, that - as anticipated - always requires a finite number of steps. This concludes the proof, establishing that *at every even N order we are able to reduce the P_N system to the form of an odd-order one with modified coefficients and with linear combinations of the unknowns.*

Moreover, clearly all the operations involved in such a proof are equivalence transformations to be operated in sequence on the original system, so that globally they give rise to an equivalence transformation, that then can be represented by left and right matrix multiplication operations: left ones correspond to Gauss pivoting to remove unwanted derivative terms from higher index rows, while right operations correspond to the sequences of required redefinitions. The question of the physical interpretation of the modified moments introduced in this reduction remains open and it will be considered in the future work.

5. Results for a two-group model

In this section the results of the calculations for a two-group model are presented. The P_N equations are solved numerically with the algorithms described in [1]. Table 4 presents the physical data employed. The data are taken from [21] and are consistent with the one-speed problem studied in [1], i.e. they refer to the same Pu-239 critical slab. Since the reference does not provide the precursors data and neutron velocities, reasonable data for the system under consideration have been adopted and are included in tables 4 and 5. The delayed fission spectra have been assumed equal to the prompt ones.

Figures 4 and 5 show the convergence trends for the fundamental eigenvalues k, γ, α and δ with 121 spatial meshes. These results are qualitatively very similar to the one-group results presented in [1], although the δ eigenvalue was not addressed there. When Mark boundary conditions are imposed, it is possible to observe that the even P_N approximations computed using the roots of the successive odd-order Legendre polynomial $P_{N+1}(\mu)$ (option A) yield eigenvalues that are larger than the reference critical one. The fact that the two approximation results envelop the correct ones is a very interesting feature that could be exploited also for acceleration purposes [22].

An intuitive explanation for this even-order P_N feature may be the fact that the directions associated to the roots of the successive odd-order P_{N+1} polynomial are more forward peaked than the ones associated to the even-order P_N, as it can be seen from the examples in table 2. As a consequence, option A effectively introduces a smaller extrapolation distance and therefore increases the boundary leakage, consistently with the fact that eigenvalues are larger than the reference values.

A simple yet physically significant proof of this fact can be derived referring to the one-speed P_1 and P_2 models, which are equivalent to diffusion. Assuming an isotropic scattering and a non-multiplying medium, for the sake of simplicity, the two models yield respectively

$$\begin{cases} \dfrac{d\phi_1}{dx} + \Sigma\phi_0 = \Sigma_s\phi_0 \\ \dfrac{1}{3}\dfrac{d\phi_0}{dx} + \Sigma\phi_1 = 0 \end{cases}, \tag{42}$$

and

$$\begin{cases} \dfrac{d\phi_1}{dx} + \Sigma\phi_0 = \Sigma_s\phi_0 \\ \dfrac{2}{3}\dfrac{d\phi_0}{dx} + \Sigma\phi_1 + \dfrac{2}{3}\dfrac{d\phi_2}{dx} = 0 \\ \dfrac{2}{5}\dfrac{d\phi_1}{dx} + \Sigma\phi_2(x) = 0 \end{cases}. \tag{43}$$

With some algebra, it is possible to find

$$\begin{cases} \dfrac{d\phi_1}{dx} = -(\Sigma - \Sigma_s)\phi_0 = -\Sigma_a\phi_0 \\ \phi_1 = -\dfrac{1}{3\Sigma}\dfrac{d\phi_0}{dx} = -D_{P_1}\dfrac{d\phi_0}{dx} \end{cases}, \tag{44}$$

and

$$\begin{cases} \dfrac{d\phi_1}{dx} = -(\Sigma - \Sigma_s)\phi_0 = -\Sigma_a\phi_0 \\ \phi_1 = -\Big(\dfrac{1}{3\Sigma} + \dfrac{4}{15}\dfrac{\Sigma_a}{\Sigma^2}\Big)\dfrac{d\phi_0}{dx} = -(D_{P_1} + D_{P_2})\dfrac{d\phi_0}{dx} \\ \phi_2 = -\dfrac{2}{5\Sigma}\dfrac{d\phi_1}{dx} = -\dfrac{2}{5}\dfrac{\Sigma_a}{\Sigma}\phi_0 \end{cases}. \tag{45}$$

Imposing Mark boundary conditions on the left boundary leads to the following equations:

$$\begin{aligned} \phi(x=0,\mu_1) &= \frac{1}{2}\phi_0(0) + \frac{3}{2}\mu_1\phi_1(0) \\ &= \frac{1}{2}\phi_0(0) - \frac{3}{2}\mu_1 D_{P_1}\left.\frac{d\phi_0}{dx}\right|_{x=0} = 0, \end{aligned} \tag{46}$$

and

$$\begin{aligned}\phi(x=0,\mu_1^*) &= \frac{1}{2}\phi_0(0) + \frac{3}{2}\mu_1^*\phi_1(0) + \frac{5}{2}\frac{1}{2}(3\mu_1^{*2}-1)\phi_2(0) \\ &= \frac{1}{2}\phi_0(0) - \frac{3}{2}\mu_1^*(D_{P_1}+D_{P_2})\left.\frac{d\phi_0}{dx}\right|_{x=0} \\ &+ \frac{5}{4}\frac{2}{5}\Big(3\mu_1^*-1\Big)\frac{\Sigma_a}{\Sigma}\phi_0(0) = 0,\end{aligned} \tag{47}$$

where μ_1 is the positive root of P_2 and μ_1^* is either the positive root of P_3 (option A) or the positive root of P_2 (option B). Similar equations can be obtained using the negative, symmetric roots for the right boundary.

Defining the extrapolated distance as the ratio between the total flux and its derivative, it is possible to get

$$d_{P_1} = 3\mu_1 D_{P_1} = \frac{\mu_1}{\Sigma}, \tag{48}$$

and

$$d_{P_2} = \frac{\frac{3}{2}\mu_1^*(D_{P_1}+D_{P_2})}{\frac{1}{2}\Big(1+(3\mu_1^{*2}-1)\frac{\Sigma_a}{\Sigma}\Big)} = \frac{\frac{\mu_1^*}{\Sigma}+\frac{4}{5}\frac{\Sigma_a}{\Sigma^2}\mu_1^*}{1+(3\mu_1^{*2}-1)\frac{\Sigma_a}{\Sigma}}. \tag{49}$$

Table 3 helps to understand the behaviour of the extrapolated distance with respect to the approximation order and the boundary condition option adopted. For a purely absorbing medium, the largest extrapolated distance is obtained with option B. On the contrary, when a non-absorbing medium is considered, option A yields the largest extrapolation distance, while option B provides the same distance as P_1. In the case of an intermediate situation, the extrapolated distances computed using the two even-order cases are similar. As it can be noticed from eq. (48) and (49), i) the extrapolation distances are fixed when P_1 and P_2 with option A are considered, ii) d_{P_1} is always smaller than d_{P_2} with the same option. These observations allow to induce that, while the convergence for the even-order P_N with option B may be case-dependent, the eigenvalue sequences computed with an even P_N with option A should always converge from the opposite side of sequences computed with an odd-order situation.

In the case the roots of the even-order Legendre polynomial $P_N(\mu)$ are considered (option B), the eigenvalues are less accurate than the ones computed with the previous P_N order, yielding almost always to higher errors,

i			
2	0.57735		
3	0.77459		
4	0.33998	0.86114	
5	0.53847	0.90618	
6	0.23862	0.66121	0.93247
7	0.40585	0.74153	0.94911

Table 2: Positive roots for some Legendre polynomials [23].

$[cm^{-1}]$		P_1	P_2 (A)	P_2 (B)
Σ_a=0	d	0.57735	0.77460	1.03923
	D	0.33333	0.60000	0.60000
	d/L	0.99999	1.00000	1.34164
Σ_a=0.5	d	0.57735	0.77460	0.80829
	D	0.33333	0.46667	0.46667
	d/L	0.70710	0.80179	0.83666
Σ_a=1	d	0.57735	0.77460	0.57735
	D	0.33333	0.33333	0.33333
	d/L	0	0	0

Table 3: Extrapolated distance d, expressed in cm, diffusion coefficient D, expressed in cm, and extrapolated distance to diffusion length ratio L, for P_1 and P_2 with options A and B for medium with $\Sigma = 1\ cm^{-1}$.

with the exception of P_2 with respect to P_1. This fact may help reconsidering P_2 as a viable alternative to P_1.

When Marshak boundary conditions are imposed, both even- and odd-order approximations lead to eigenvalues that are smaller than the reference, with some notable exceptions regarding P_2 and P_4, in analogy with what observed in the one-group case. The reader is referred to [1] for a possible justification of this peculiar behaviour.

For both Mark and Marshak cases, the α eigenvalue results show absolute errors that are much larger than for the other cases, where the error is expressed in pcm. It should be remarked though that, in the transport equation, α is divided by the neutron velocity, which makes the time capture

term very small indeed.

ν_1	Σ_1	$\Sigma_{f,1}$	$\Sigma_{1\to1}$	$\Sigma_{1\to2}$	χ_1	$\mathtt{v_1}^{-1}$
3.1	0.22080	0.09360	0.07920	0.04320	0.575	4.53849E-08
ν_2	Σ_2	$\Sigma_{f,2}$	$\Sigma_{2\to1}$	$\Sigma_{2\to2}$	χ_2	$\mathtt{v_2}^{-1}$
2.93	0.33600	0.08544	0	0.23616	0.425	2.18142E-06

Table 4: Material data for the case study adopted to investigate the rôle of boundary conditions and parity order. The data are taken from ref. [21] (two-group Pu-239 slab). The data have their usual dimensions: cross sections are expressed in cm^{-1}, the inverse of the velocity is expressed in s/cm while the number of neutrons emitted by fission and the fission spectra are dimensionless. Scattering is assumed isotropic. The critical thickness is equal to 3.5912040 cm.

i	λ_i $[s^{-1}]$	β_i $[-]$
1	0.0133826	$8.86440 \cdot 10^{-05}$
2	0.0308055	$6.75625 \cdot 10^{-04}$
3	0.1170030	$5.37368 \cdot 10^{-04}$
4	0.3066840	$1.22693 \cdot 10^{-03}$
5	0.8780670	$7.10462 \cdot 10^{-04}$
6	2.9378800	$2.50592 \cdot 10^{-04}$

Table 5: Delayed neutron precursors family data for the cases presented throughout the paper.

Tables 6 and 7 show the fundamental eigenvalues for all the formulations considered in this paper computed with relatively high-order P_N approximations. The purpose of such tables is two-fold: i) observing the convergence trend shown in figs. 4 and 5 for more accurate approximations, ii) providing reference results, since, to the authors' knowledge, high-order P_N calculations for these eigenvalues are completely missing in the literature.

It is interesting to notice that up to P_{202} adopting option A the eigenvalues k, γ and δ are still larger than the reference, while starting from P_{401} both options A and B yield values that are smaller than the reference, suggesting that there is a certain order for which the error is minimum. A similar behaviour occurs also for α and ω, although the latter keeps always the

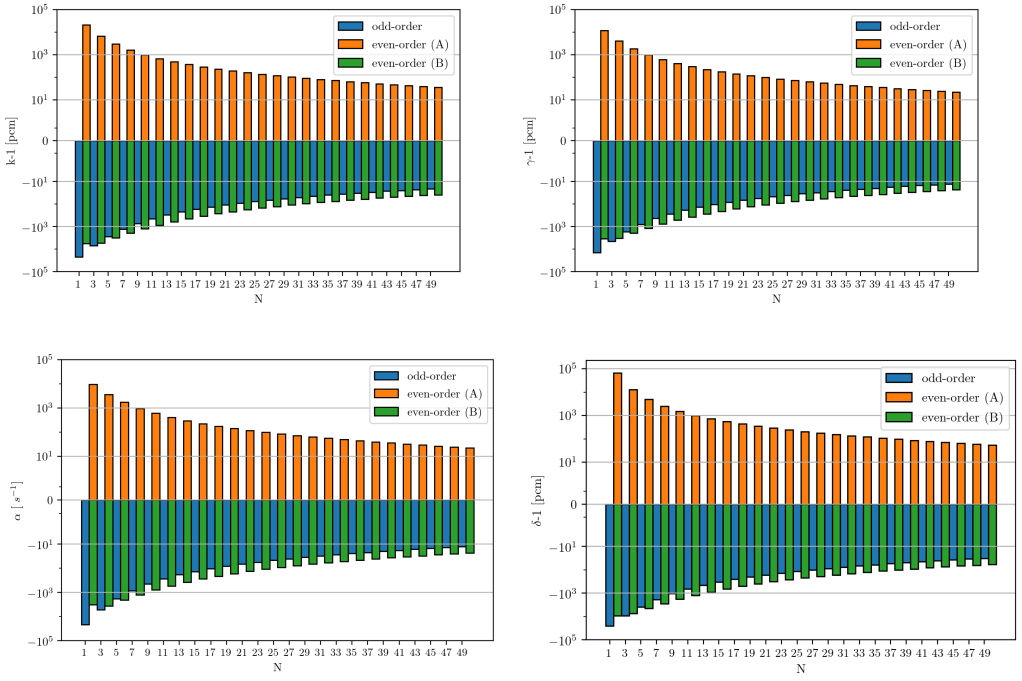

Figure 4: Convergence of the fundamental values for k, γ, α and δ, adopting Mark boundary conditions.

same sign. The justification of this trend may be the lack of accuracy in the critical thickness of the slab, which is provided in [21] with only 5 significant digits. Another interesting feature that can be observed in the tables is the fact that ω is much closer to 0 than the prompt time eigenvalue α. This behaviour can be justified considering the presence of the clusters of delayed eigenvalues, which force the fundamental eigenvalue to be larger than -λ_1, consistently with elementary nuclear reactor physics and also more sophisticated approaches [24, 25].

Figure 6 shows the fundamental eigenfunctions and the associated spectral index (ratio between fast and thermal distributions) for a close-to-critical and two off-critical cases, in order to appreciate the behaviour of the harmonics with respect to the eigenvalue formulations. The distributions have been computed using P_{51} with Mark boundary conditions and 121 spatial meshes. For the sub- and super-critical cases the critical thickness has been halved and doubled, respectively. As expected, the eigenfunctions cannot be

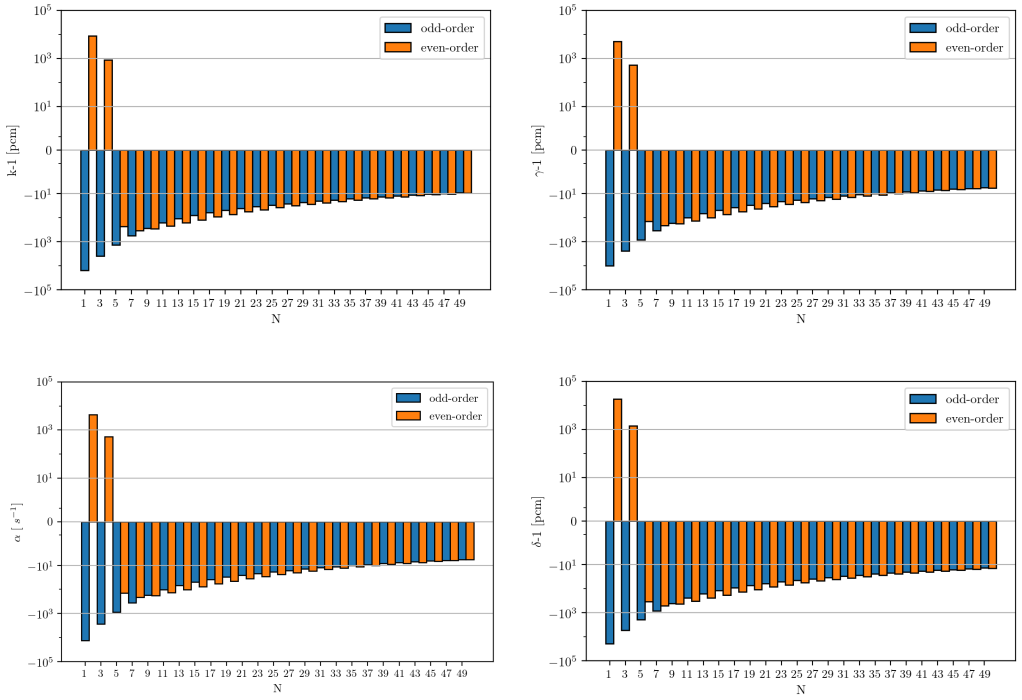

Figure 5: Convergence of the fundamental values for k, γ, α and δ, adopting Marshak boundary conditions.

easily distinguished when the system is very close to criticality, while their behaviour is quite different in the sub- and super-critical cases. The direct inspection of the graphs for the spectral indices shows that even far away from the boundaries no space-energy separability [5] is shown. This is consistent with the small optical dimensions of the systems adopted in the reference cases.

6. Time eigenvalue spectra

In this section we present the spectra of the time eigenvalues α and ω. The spatially discretised version of the P_N equations leads to a finite set of eigenvalues. The main goal of this section is to provide an idea of the effect of the different P_N approximation orders on the pattern of the eigenvalue spectrum.

N	BC option	k [-]	γ [-]	δ [-]	α $[s^{-1}]$	ω $[s^{-1}]$
201		0.9999678725	0.9999803980	0.9999518269	-8.6828282535	-0.0008211782
202	B	0.9999622839	0.9999769882	0.9999434487	-10.1932439604	-0.0009593605
	A	1.0000077738	1.0000047430	1.0000116573	2.1009131707	0.00020570523
401		0.9999755828	0.9999851023	0.9999633873	-6.5990034889	-0.0006282912
402	B	0.9999758138	0.9999852433	0.9999637337	-6.5365820922	-0.0006224728
	A	0.9999879542	0.9999926505	0.9999819373	-3.2554890613	-0.0003133042
601		0.9999772297	0.9999861072	0.9999658567	-6.1538958367	-0.0005867509
602	B	0.9999777461	0.9999864223	0.9999666310	-6.0143364578	-0.0005737018
	A	0.9999835466	0.9999899613	0.9999753284	-4.4466753337	-0.0004263066
801		0.9999779404	0.9999865408	0.9999669223	-5.9618235960	-0.0005687884
802	B	0.9999783105	0.9999867666	0.9999674772	-5.8618085744	-0.0005594263
	A	0.9999817887	0.9999888887	0.9999726924	-4.9217874910	-0.0004711359
1001		0.9999783238	0.9999867747	0.9999674972	-5.8582115034	-0.0005590894

Table 6: Values of fundamental k, γ, δ, α and ω for various P_N orders and Mark boundary conditions using 121 spatial meshes.

Figure 7 compares the spectra computed with P_1, P_3 and P_7 when only prompt, α, or prompt and delayed neutrons, ω, are considered. The difference between the two cases cannot be appreciated *ictu oculi*, as both the distribution and the values in the complex plane are approximately the same, except for the region around the origin, that for scale reasons is not well resolved. The difference between the two spectra in this region can be observed in fig. 8.

The prompt eigenvalues are by far larger than the delayed ones, which cluster as the roots of the in-hour equations, approaching the values -λ_i, $i = 1, ..., R$ [7]. Also in the two-group case, it is possible to observe that the eigenvalues are distributed in different sets, which can be interpreted referring to the relationship with a $N + 1$ discrete directions model. Moving from one odd approximation to the next odd one, the eigenvalues present a new pattern involving the addition of two pitches towards the negative portion of the real axis. Since the roots of the Legendre polynomials are symmetric with respect

N	k [-]	γ [-]	δ [-]	α $[s^{-1}]$	ω $[s^{-1}]$
201	0.9999757396	0.9999851980	0.9999636225	-6.5566304223	-0.0006243417
202	0.9999798359	0.9999876973	0.9999697648	-5.4495411470	-0.0005207699
401	0.9999781586	0.9999866739	0.9999672495	-5.9028576703	-0.0005632693
402	0.9999804984	0.9999881015	0.9999707578	-5.2704980078	-0.0005039507
601	0.9999786556	0.9999869772	0.9999679947	-5.7685302820	-0.0005506890
602	0.9999799800	0.9999877852	0.9999699804	-5.4106092928	-0.0005171149
801	0.9999788751	0.9999871111	0.9999683238	-5.7092086649	-0.0005451298
802	0.9999796438	0.9999875801	0.9999694764	-5.5014640514	-0.0005256448
1001	0.9999789882	0.9999871801	0.9999684934	-5.6786445762	-0.0005422648

Table 7: Values of fundamental k, γ, δ, α and ω for various P_N orders and Marshak boundary conditions using 121 spatial meshes.

to the real axis origin, also the eigenvalues are symmetric with respect to the real axis in the complex plane.

The impact of the even-order approximation on the time delayed spectrum can be appreciated in fig. 9. As it can be clearly seen, the overall shape of the spectrum is preserved, as expected, with respect to the preceding odd-order. Therefore, the only effect is a slight distortion in the eigenvalues distribution.

7. Density eigenvalue spectrum

This section is devoted to investigate on the physical meaning of the most exotic and less studied eigenvalue among the ones presented in this paper, i.e. the effective density (or streaming) one. We start considering a purely absorbing medium and progressively adding scattering and fission, leading to four cases whose data are summarized in Table 8.

Figure 10 shows the spectra for the purely absorbing medium (case A in table 8), evaluated with increasing odd- and even-orders. It is of paramount importance to remark that, while the odd-order spectra are fully described by these plots, the even-order cases are only a zoom that excludes a set of extremely large eigenvalues ($\sim 10^{15}$). The appearance of such eigenvalues may be justified by the fact that the streaming operator, whose eigenvalue

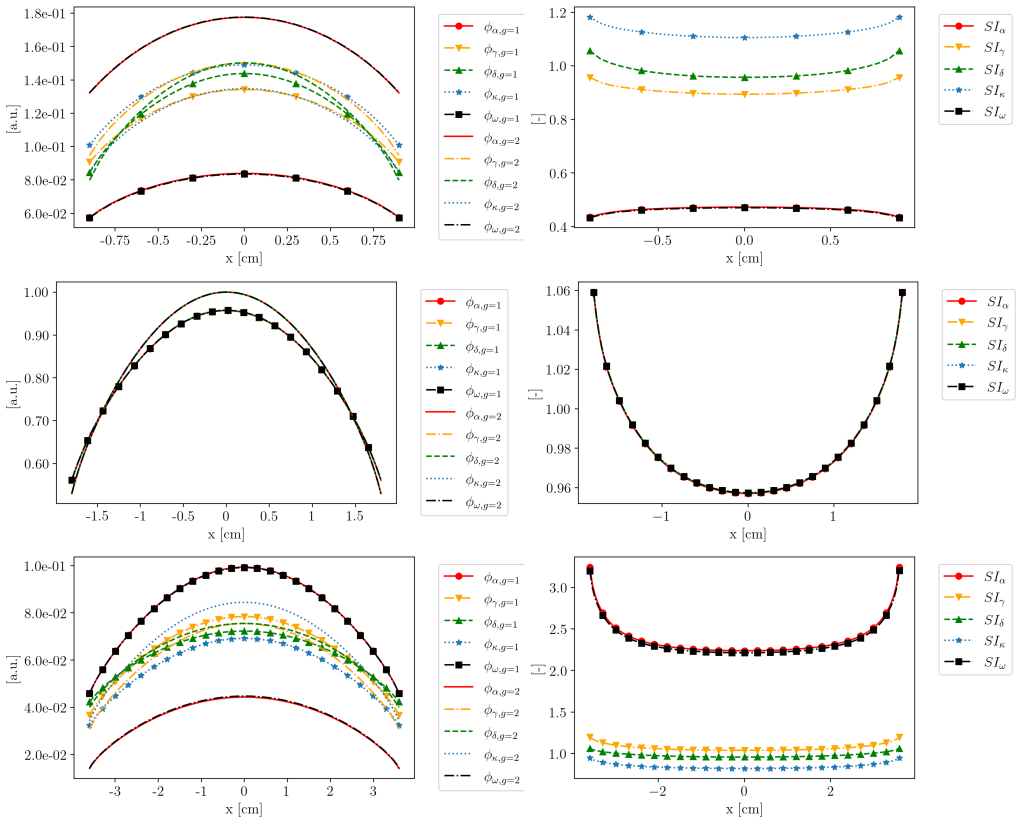

Figure 6: Fundamental eigenfunctions (left) and spectral indeces (right) for the five eigenproblem formulations in sub-critical (k=0.61421, top), close-to-critical (k=0.99976, center) and super-critical (k=1.52469, bottom), using a P_{51} approximation with Mark boundary conditions using 100 spatial meshes.

is δ itself, is singular when the even-order P_N is employed, consistently with the proof provided in section 4. This mathematical justification may be strengthened also by a physical fact: in analogy with the S_N approach, even-order approximations introduce a streaming direction that is parallel to the slab boundaries, $\mu_{N/2+1} = 0$. Neutrons streaming along this direction would never leak out of the system, leading to an algebraic equation that may be expressed using the equivalent S_{N+1} model [26]

$$\mu_{N/2+1} \frac{\partial \phi(x, \mu_{N/2+1})}{\partial x} = -\frac{1}{\delta} \Sigma \phi(x, \mu_{N/2+1}) = 0. \tag{50}$$

Assuming Σ and ϕ are non-zero, eq. (50) can be satisfied only if $\delta \to \infty$.

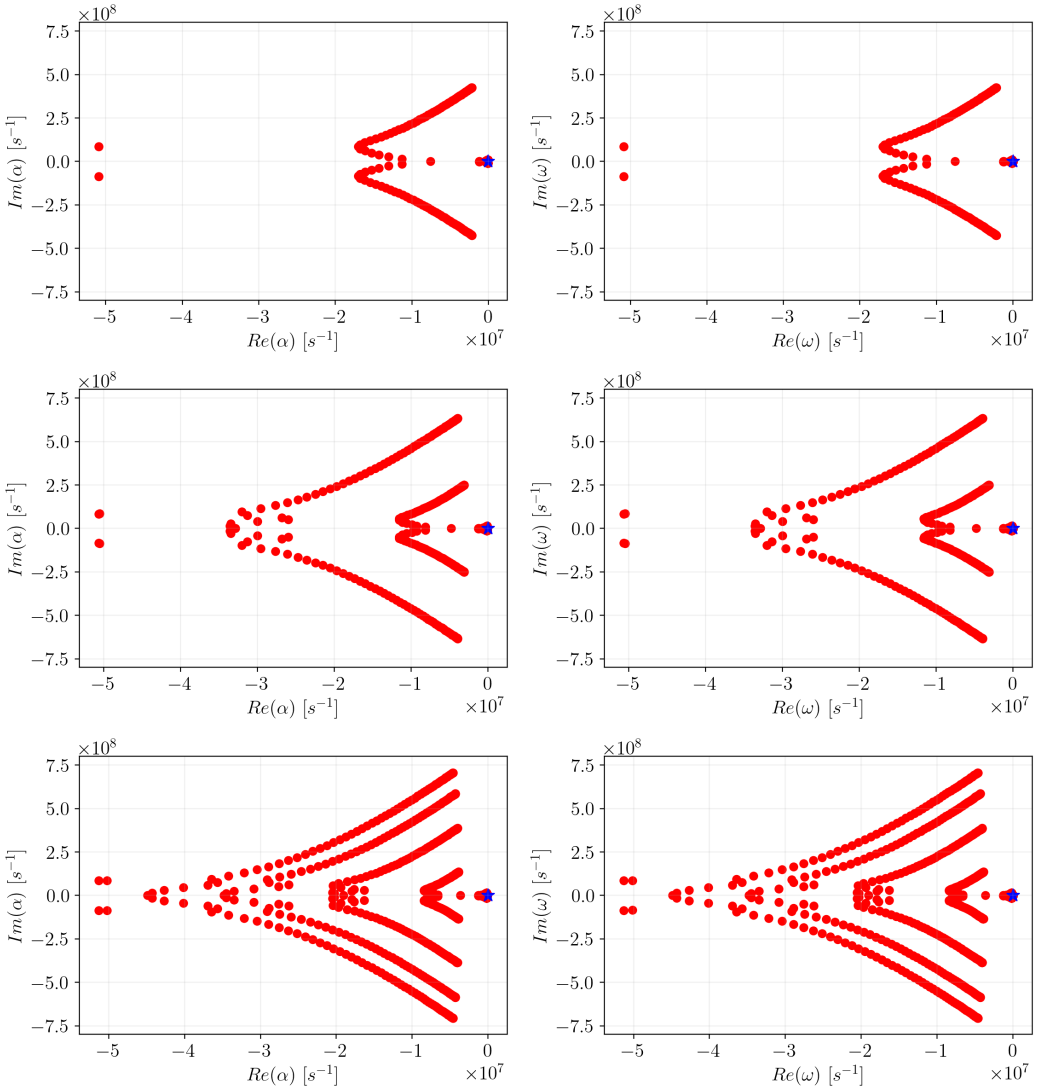

Figure 7: Spectra of α (left) and ω (right) eigenvalues for a slab in the two-group energy model for P_1, P_3 and P_7 approximations (from top to bottom). The blue star is the fundamental eigenvalue.

Similarly to previous eigenvalue formulations, the increasing P_N order introduces more patterns in the δ spectrum, while the odd-even order comparison results into a distortion of such patterns.

Figure 11 shows that δ eigenvalues can be either positive or negative:

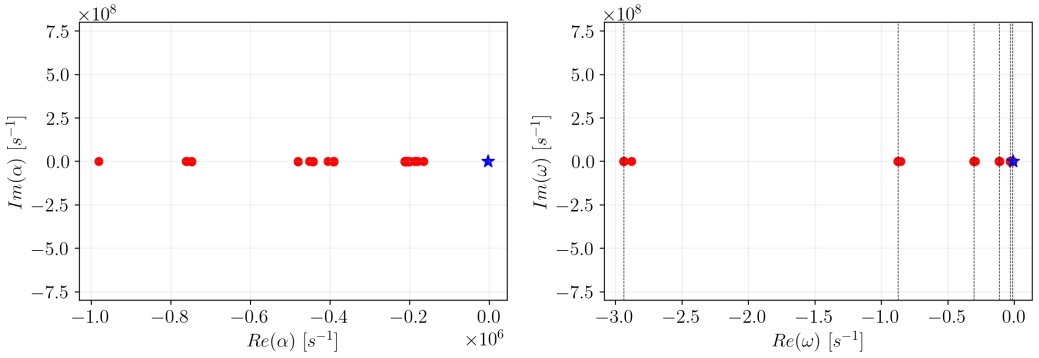

Figure 8: Spectra of α (left) and ω (right) eigenvalues for a slab in the two-group energy model for P_7 approximation. The blue star is the fundamental eigenvalue, while the black dashed lines are located at -λ_1, ..., -λ_6.

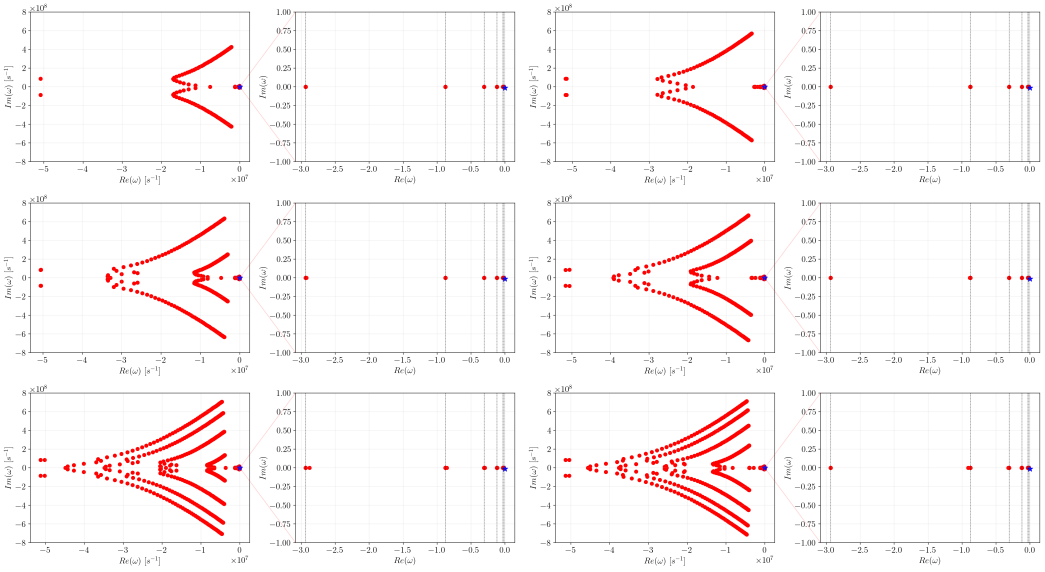

Figure 9: Spectra of ω eigenvalues for a slab in the two-group energy model for P_1, P_2, P_3, P_4, P_7 and P_8 approximations (from left to right and from top to bottom). The blue star is the fundamental eigenvalue. Columns 2 and 4 zoom the spectra near the origin.

this is due to the particular rôle played by this eigenvalue, which modifies all collision terms that give a competing contribution in the balance equation, as previously observed.

The introduction of the δ eigenvalue opens several theoretical problems

Case	$\Sigma_{s,0}$	Σ_f	ν
A	0	0	0
B	0	0.05	2.5
C	0	0.5	2.5
D	0.5	0.5	0

Table 8: Material data for the cases adopted to investigate the δ eigenvalue spectra in the one-speed formulation. Cross sections are expressed in cm^{-1}. The medium is characterized by Σ=1 cm^{-1}. The slab thickness is equal to 3.5912040 cm.

and intricacies in its physical interpretation. In a further work, these aspects will be considered in some more detail.

8. Conclusions

In this paper, all the known eigenvalue formulations of the neutron transport equation have been addressed in the framework of the plane geometry P_N approximation. In addition to the classical formulations, i.e. multiplication (k), collision (γ) and prompt time (α) eigenvalues, also the density eigenvalue δ and the delayed time eigenvalue ω have been analysed.

The first part of the paper presents a semi-analytical approach for the calculation of the one-group α spectrum in the idealised case of a purely absorbing medium. Remarkably, this is a very particular situation because only thanks to the use of a Legendre expansion of the transport equation it is possible to obtain an α spectrum, which would not be present in the same limit for the exact transport equation or its discrete ordinates formulation. Then, the same approach is used to study the spectrum modification when scattering and fission are considered.

Afterwards, we provide a proof of the fact that it is possible, in general, to cast an even-order P_N equation in plane geometry into an equivalent, yet different, odd-order formulation. This evidence justifies the historical preference, within the transport community, for the odd-order P_N approximations rather than the successive even-order one.

In the second part of the paper, we study the angular convergence behaviour for a Pu-239 critical slab in a two-group model , obtaining trends that are very similar to the ones already observed in [1] for a one-group problem, using both Mark and Marshak boundary conditions. The impact of the

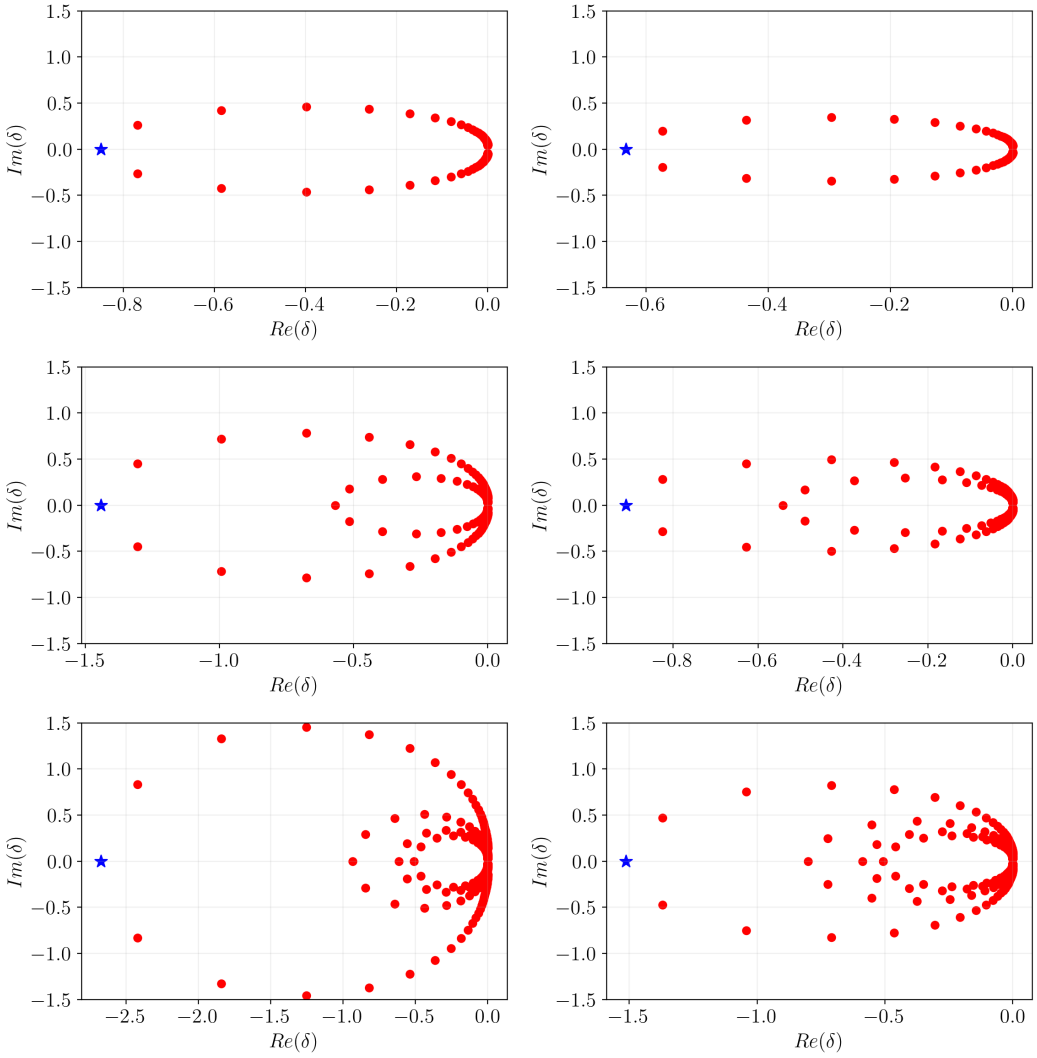

Figure 10: Spectra of δ eigenvalues for a slab in a one-group model for P_1, P_2, P_3, P_4, P_7 and P_8 approximations in absence of scattering, with Mark boundary conditions. The blue star is the fundamental eigenvalue. The plots on the right (even-order P_N) are zoomed in order to exclude very large eigenvalues that appear in the spectrum.

P_N order on the eigenvalues convergence is studied also for relatively high N, showing once again the same trend. These results highlight a very interesting and useful feature of the eigenvalue sequences when Mark boundary conditions are imposed. As a matter of fact, both odd- and even-order sequences

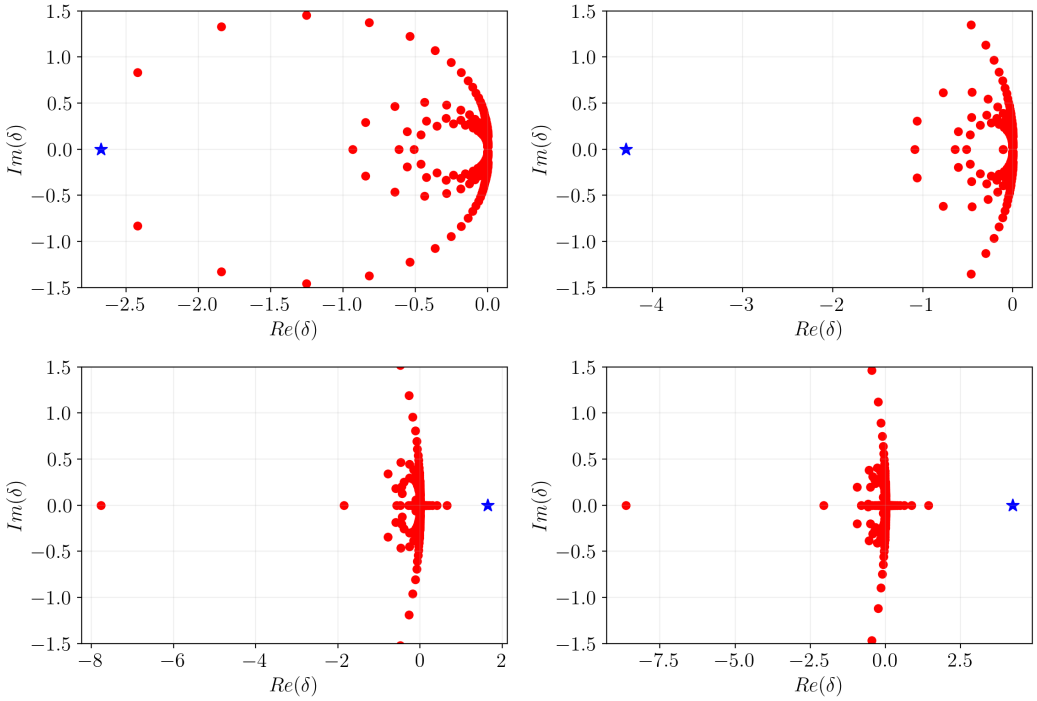

Figure 11: Spectra of δ eigenvalues for a slab in a one-group model for P_7 approximations, with Mark boundary conditions. Top-left is case A, top-right is case B, bottom-left is case C and bottom-right is case D. The blue star is the fundamental eigenvalue.

converge from opposite sides to the reference values when the angular flux is made to vanish in the directions corresponding to the roots of the Legendre polynomial $P_{N+1}(\mu)$, where N is the approximation order adopted, even or odd. This property discloses the possibility to get very accurate estimates of the eigenvalues using suitable acceleration techniques that could thus benefit also from even-order approximations.

Finally, the spectra of ω and δ are studied with respect to the N approximation order. While the ω spectrum is not much affected when an even-order P_N is adopted instead of an odd-order one, the δ spectrum presents very large, spurious eigenvalues, which may be physically explained thanks to the P_N-S_{N+1} equivalence.

Future work will be devoted to study eigenvalue convergence acceleration and to extend this analysis also to reflected systems, in order to evaluate the influence of non-multiplying media on the different eigenvalue spectra,

especially δ and ω. Furthermore, a deeper analysis of the mathematical features and physical meaning of the density eigenvalue is necessary to better understand its characteristics and to open the possibility of its application for reactor physics.

In the future work we plan also to investigate further formulations of the eigenvalue problem, such as the capture eigenvalue, involving a modification only on the capture cross sections. This formulation would be of practical interest for applications in the field of control engineering of nuclear reactors. At last, other transport models should be investigated, e.g. discrete ordinates and models based on the integral transport equation.

Appendix A. Even to odd reduction as equivalence transformation

Two matrix $\hat{A}$ and $\hat{B}$ are said to be equivalent if there exist invertible matrices $\hat{Q}$ and $\hat{P}$ such that

$$\hat{B} = \hat{Q}^{-1} \cdot \hat{A} \cdot \hat{P} \,. \tag{A.1}$$

Equivalent matrices represent the same linear transformation $V \longrightarrow W$ with two different choices of the basis in V and in W; the set of operations known as Gauss elimination process is an example of equivalence transformation.

Here we explain how to build the matrices necessary to reduce an even P_N system to its equivalent P_{N-1}, as it was outlined in the main text. First, we convert the original system to a purely algebraic one by taking its Laplace transform. Then, the first operation is to find the solution for the highest angular flux moment: this corresponds to finding the sequence of row operations enabling to remove any dependence from the complex Laplace frequency ω. This can be done by recursively eliminating terms of the last line depending on ω by using, to this purpose, the row displaying an ω dependence as the last non-vanishing element. The fact that this is always possible is a trivial consequence of the tridiagonal structure of the P_N system.

Every operation of such sequence is an elementary operation from the Gauss reduction set and it has unitary determinant; moreover, they commute one with each other. At the end of the sequence, the last line does not depend on ω and its last element is equal to 1. Then, we use again Gauss elimination to remove the highest angular flux moment from the rest of the system, by using the modified last line.

To make the element B_{mn} of a given matrix vanish, we need simply to subtract from its m-th line the k-th one multiplied by $-B_{mn}/B_{kn}$, provided naturally that $B_{kn} \neq 0$: this is done by left multiplication by an identity matrix of the same dimension of the number of rows in $\hat{B}$ - in such a way that the matrix product is properly defined - with also a $1 - B_{mn}/B_{kn}$ term at the k-th column. This has the side effect of changing also other elements of the same row: however, the number of elements in the row that depends on ω is reduced by 1. In such a way we conclude to be always able to find a matrix equivalent to the original one depending (linearly) on ω only on the super and subdiagonals.

However, the procedure is not terminated because other terms independent on ω can remain on the line under examination: to get rid of them - leaving only a tridiagonal subsystem with the required features - we resort to a redefinition of the unknowns. This can be done by right multiplying by a proper matrix.

Having sketched the procedure, we show it explicitly at work in the case of the reduction of $\hat{P}_6$, which begins considering the 7×7 matrix

$$\hat{P}_6 = \begin{pmatrix} \mathrm{a} & \omega & 0 & 0 & 0 & 0 & 0 \\ \frac{\omega}{3} & 1 & \frac{2\omega}{3} & 0 & 0 & 0 & 0 \\ 0 & \frac{2\omega}{5} & 1 & \frac{3\omega}{5} & 0 & 0 & 0 \\ 0 & 0 & \frac{3\omega}{7} & 1 & \frac{4\omega}{7} & 0 & 0 \\ 0 & 0 & 0 & \frac{4\omega}{9} & 1 & \frac{5\omega}{9} & 0 \\ 0 & 0 & 0 & 0 & \frac{5\omega}{11} & 1 & \frac{6\omega}{11} \\ 0 & 0 & 0 & 0 & 0 & \frac{6\omega}{13} & 1 \end{pmatrix} . \tag{A.2}$$

A first sequence of 3 Gauss eliminations enables to find the solution for ϕ_6

$$\hat{L}_3 \cdot \hat{L}_2 \cdot \hat{L}_1 \cdot \hat{P}_6 = \begin{pmatrix} a & \omega & 0 & 0 & 0 & 0 & 0 \\ \frac{\omega}{3} & 1 & \frac{2\omega}{3} & 0 & 0 & 0 & 0 \\ 0 & \frac{2\omega}{5} & 1 & \frac{3\omega}{5} & 0 & 0 & 0 \\ 0 & 0 & \frac{3\omega}{7} & 1 & \frac{4\omega}{7} & 0 & 0 \\ 0 & 0 & 0 & \frac{4\omega}{9} & 1 & \frac{5\omega}{9} & 0 \\ 0 & 0 & 0 & 0 & \frac{5\omega}{11} & 1 & \frac{6\omega}{11} \\ -\frac{16a}{65} & 0 & \frac{8}{13} & 0 & -\frac{54}{65} & 0 & 1 \end{pmatrix} , \tag{A.3}$$

that, as anticipated, informs us that ϕ_6 is not an unknown, being simply

$$-\frac{16a}{65}\phi_0(x) + \frac{8}{13}\phi_2(x) - \frac{54}{65}\phi_4(x) + \phi_6(x) = 0 \,, \tag{A.4}$$

thanks to a sequence of 3 successive Gauss eliminations $\hat{L}_1, \hat{L}_2$ and $\hat{L}_3$ to remove sequentially the ω dependencies from row $m = 6$, column $n = 5$ using the pivot at line $m = 4$, then the induced dependency at row $m = 6$, column $n = 3$ with the pivot in line $m = 2$, finally the one in row $m = 6$, column $m = 1$. This has been accomplished by the 3 matrices $\hat{L}_1, \hat{L}_2$ and $\hat{L}_3$, globally resulting into the transformation:

$$\hat{L}_3 \cdot \hat{L}_2 \cdot \hat{L}_1 = \begin{pmatrix} 1 & 0 & 0 & 0 & 0 & 0 & 0 \\ 0 & 1 & 0 & 0 & 0 & 0 & 0 \\ 0 & 0 & 1 & 0 & 0 & 0 & 0 \\ 0 & 0 & 0 & 1 & 0 & 0 & 0 \\ 0 & 0 & 0 & 0 & 1 & 0 & 0 \\ 0 & 0 & 0 & 0 & 0 & 1 & 0 \\ -\frac{16}{65} & 0 & \frac{8}{13} & 0 & -\frac{54}{65} & 0 & 1 \end{pmatrix} . \tag{A.5}$$

The expression in eq. (A.4) can be replaced - by using a similar $\hat{L}_4$ matrix into the $m = 5$ equation to remove the ω dependence from the last term of row $m = 5$: to do this, clearly we have to multiply the row $m = 6$ by ω, so modifying the dependency on ω of the transformed matrix:

$$\hat{L}_4 \cdot \hat{L}_3 \cdot \hat{L}_2 \cdot \hat{L}_1 \cdot \hat{P}_6 = \begin{pmatrix} a & \omega & 0 & 0 & 0 & 0 & 0 \\ \frac{\omega}{3} & 1 & \frac{2\omega}{3} & 0 & 0 & 0 & 0 \\ 0 & \frac{2\omega}{5} & 1 & \frac{3\omega}{5} & 0 & 0 & 0 \\ 0 & 0 & \frac{3\omega}{7} & 1 & \frac{4\omega}{7} & 0 & 0 \\ 0 & 0 & 0 & \frac{4\omega}{9} & 1 & \frac{5\omega}{9} & 0 \\ \frac{96a\omega}{715} & 0 & -\frac{48\omega}{143} & 0 & \frac{59\omega}{65} & 1 & 0 \\ -\frac{16a}{65} & 0 & \frac{8}{13} & 0 & -\frac{54}{65} & 0 & 1 \end{pmatrix} . \tag{A.6}$$

Remarkably, $\hat{L}_4$ does not commute with $\hat{L}_3 \cdot \hat{L}_2 \cdot \hat{L}_1$: it has been inserted on the left because this transformation must happen after the others. We now have to play the same game to remove the first two ω dependencies from line $m = 5$, the last being the required one.

With other two transformations $\hat{L}_5, \hat{L}_6$ (with pivot respectively at rows

$m = 0$ and $m = 3$), this can be easily done, yielding:

$$\hat{L}_6 \cdot \hat{L}_5 \cdot \hat{L}_4 \cdot \hat{L}_3 \cdot \hat{L}_2 \cdot \hat{L}_1 \cdot \hat{P}_6 \;=\; \tag{A.7}$$
$$\begin{pmatrix} a & \omega & 0 & 0 & 0 & 0 & 0 \\ \frac{\omega}{3} & 1 & \frac{2\omega}{3} & 0 & 0 & 0 & 0 \\ 0 & \frac{2\omega}{5} & 1 & \frac{3\omega}{5} & 0 & 0 & 0 \\ 0 & 0 & \frac{3\omega}{7} & 1 & \frac{4\omega}{7} & 0 & 0 \\ 0 & 0 & 0 & \frac{4\omega}{9} & 1 & \frac{5\omega}{9} & 0 \\ 0 & -\frac{288a}{715} & 0 & \frac{448a}{715} + \frac{112}{143} & \frac{256a\omega}{715} + \frac{969\omega}{715} & 1 & 0 \\ -\frac{16a}{65} & 0 & \frac{8}{13} & 0 & -\frac{54}{65} & 0 & 1 \end{pmatrix}.$$

Here, as anticipated in the main text, the suggestion is to redefine the variable $\phi_5(x)$ in such a way to remove the unwanted terms in columns $n = 1$ and $n = 3$; this can be done by the *right multiplication* by $\hat{R}_1$

$$\hat{R}_1 = \begin{pmatrix} 1 & 0 & 0 & 0 & 0 & 0 & 0 \\ 0 & 1 & 0 & 0 & 0 & 0 & 0 \\ 0 & 0 & 1 & 0 & 0 & 0 & 0 \\ 0 & 0 & 0 & 1 & 0 & 0 & 0 \\ 0 & 0 & 0 & 0 & 1 & 0 & 0 \\ 0 & \frac{288a}{715} & 0 & -\frac{448a}{715} - \frac{112}{143} & 0 & 1 & 0 \\ 0 & 0 & 0 & 0 & 0 & 0 & 1 \end{pmatrix}, \tag{A.8}$$

which again is manifestly non-singular. The result is

$$\begin{pmatrix} a & \omega & 0 & 0 & 0 & 0 & 0 \\ \frac{\omega}{3} & 1 & \frac{2\omega}{3} & 0 & 0 & 0 & 0 \\ 0 & \frac{2\omega}{5} & 1 & \frac{3\omega}{5} & 0 & 0 & 0 \\ 0 & 0 & \frac{3\omega}{7} & 1 & \frac{4\omega}{7} & 0 & 0 \\ 0 & \frac{32a\omega}{143} & 0 & \frac{4\omega}{429} - \frac{448a\omega}{1287} & 1 & \frac{5\omega}{9} & 0 \\ 0 & 0 & 0 & 0 & \frac{256a\omega}{715} + \frac{969\omega}{715} & 1 & 0 \\ -\frac{16a}{65} & 0 & \frac{8}{13} & 0 & -\frac{54}{65} & 0 & 1 \end{pmatrix}. \tag{A.9}$$

We proceed as outlined by eliminating the ω dependent term at row $m = 4$, column $n = 1$; by inspection this yields to the replacement (matrix $\hat{R}_2$, not explicitly shown)

$$-\frac{80a}{143}\phi_2 + \phi_4 = \Phi_4, \tag{A.10}$$

in such a way to recast also the row $m = 4$ into the desired form. However, this substitution modifies also the $m = 5, 6$ equations that depend on ϕ_4,

forcing to repeat the elimination procedure from row $m = 5$ where a new term proportional to ϕ_2 appeared, but, and *this ensures the process is finite*, with a lower number of elements to be modified:

$$\left(\frac{4096a^2\omega}{20449} + \frac{15504a\omega}{20449}\right)\phi_2 + \left(\frac{256a\omega}{715} + \frac{969\omega}{715}\right)\Phi_4 + \Phi_5. \tag{A.11}$$

The term proportional to ϕ_2 must be eliminated using the pivot in line $m = 3$, then a new variable is introduced through

$$-\frac{((112a(969+256a))}{(143(429+320a)))}\phi_3 + \Phi_5 = \Psi_5\,, \tag{A.12}$$

where Φ_5 was introduced using the matrix $\hat{R}_1$. To summarize, the original $\hat{P}_6$ matrix is transformed into the equivalent

$$\hat{P}_6' = \begin{pmatrix} a & \omega & 0 & 0 & 0 & 0 & 0 \\ \frac{\omega}{3} & 1 & \frac{2\omega}{3} & 0 & 0 & 0 & 0 \\ 0 & \frac{2\omega}{5} & 1 & \frac{3\omega}{5} & 0 & 0 & 0 \\ 0 & 0 & \frac{(320a+429)\omega}{1001} & 1 & \frac{4\omega}{7} & 0 & 0 \\ 0 & 0 & 0 & \frac{4(3-220a)\omega}{1287} + \frac{560a(256a+969)\omega}{1287(320a+429)} & 1 & \frac{5\omega}{9} & 0 \\ 0 & 0 & 0 & 0 & \frac{3(256a+969)\omega}{5(320a+429)} & 1 & 0 \\ -\frac{16a}{65} & 0 & \frac{8}{13} - \frac{864a}{1859} & 0 & -\frac{54}{65} & 0 & 1 \end{pmatrix}, \tag{A.13}$$

where the last line expresses explicitly the solution for ϕ_6 and the remaining part is a $\hat{P}_5$-like matrix with modified coefficients. At last, we remark that, after this procedure, the interpretation of the new flux moments is not trivial because of the sequence of redefinitions that has been carried on.

References

[1] N. Abrate, M. Burrone, S. Dulla, P. Ravetto, and P. Saracco. Eigenvalue formulations for the P_N approximation to the neutron transport equation. *Journal of Computational and Theoretical Transport*, 49:1–23, 2020.

[2] N. Abrate, B.D. Ganapol, S. Dulla, P. Ravetto, P. Saracco, and A. Zoia. Convergence acceleration aspects in the solution of the P_N neutron transport eigenvalue problem. *International Conference M&C 2021, Rayleigh*, 2021.

[3] R. V. Meghreblian and D. K. Holmes. *Reactor Analysis*. McGraw-Hill, New York, 1960.

[4] G. Palmiotti and M. Salvatores. Calcule des harmonique en géometrie hexagonale. *Bulletin de la direction des études et recherches, Serie A*, 1:43–60, 1985.

[5] A.M Weinberg and E.P. Wigner. *The Physical Theory of Neutron Chain Reactors*. University of Chicago Press, Chicago, 1958.

[6] A. Zoia, E. Brun, and F. Malvagi. Alpha eigenvalue calculations with TRIPOLI-4®. *Annals of Nuclear Energy*, 63:276 – 284, 2014.

[7] A. F. Henry. The application of inhour modes to the description of non-separable reactor transients. *Nuclear Science and Engineering*, 20:338–351, 1964.

[8] B. Davison. *Neutron Transport Theory*. University Press, Oxford, 1958.

[9] D. G. Cacuci, Y. Ronen, Z. Shayer, J. J. Wagschal, and Y. Yeivin. Eigenvalue-dependent neutron energy spectra: definitions, analyses, and applications. *Nuclear Science and Engineering*, 81:432–442, 1982.

[10] J. Bussac and P. Reuss. *Traité de neutronique*. Hermann, Paris, 1985.

[11] A. Barbarino, S. Dulla, and P. Ravetto. Integral neutron transport and new computational methods: a review. In C. Constanda, B. Bodmann, and H. Velho, editors, *Integral Methods in Science and Engineering*. Birkhäuser, New York, NY, 2013.

[12] J.C. Mark. The spherical harmonics method, Part I, Atomic Energy Report 92, National Research Council of Canada, 1944.

[13] J.C. Mark. The spherical harmonics method, Part II, Atomic Energy Report 97, National Research Council of Canada, 1945.

[14] R.E. Marshak. Note on the spherical harmonics method as applied to the Milne problem for a sphere. *Physical Review*, 71:443–446, 1947.

[15] Wolfram Research, Inc. Mathematica, Version 12.2. Champaign, IL, 2020.

[16] W. Frank and P. von Brentano. Classical analogy to quantum mechanical level repulsion. *American Journal of Physics*, 62:706, 1994.

[17] K.M. Case and P.L. Zweifel. *Linear Transport Theory*. Addison-Wesley, Reading, 1967.

[18] G.W. Faris. P_N approximation for frequency-domain measurements in scattering media. *App. Optics*, 44:2058, 2005.

[19] G. Y. Rumyantsev. Boundary conditions in the spherical harmonic method. *Journal of Nuclear Energy*, 16:111, 1962.

[20] R. Sanchez. On P_N interface and boundary conditions. *Nuclear Science and Engineering*, 177(1):19–34, 2014.

[21] A. Sood, R. A. Forster, and D. K. Parsons. Analytical benchmark test set for criticality code verification. *Progress in Nuclear Energy*, 42:55–106, 2003.

[22] B.D. Ganapol. What is convergence acceleration anyway? In C. Constanda, B. Bodmann, and H. Velho, editors, *Integral Methods in Science and Engineering*. Birkhäuser, New York, NY, 2013.

[23] M. Abramowitz and I. A. Stegun. *Handbook of Mathematical Functions with Formulas, Graphs, and Mathematical Tables*. Dover, New York, 1964.

[24] R. Sanchez, D. Tomatis, I. Zmijarevic, and H. G. Joo. Analysis of alpha modes in multigroup diffusion. *Nuclear Engineering and Technology*, 49:1259–1268, 2017.

[25] R. Sanchez and D. Tomatis. Analysis of alpha modes in multigroup transport. *International Conference M&C 2019, Portland*, 2019.

[26] S. I. Heizler and P. Ravetto. SP_2 - asymptotic P_1 equivalence. *Transport Theory and Statistical Physics*, 41(3-4):304–324, 2012.